



Engineering

University of Windsor

SAE AERO DESIGN

Capstone Design MECH-4200

Faculty of Engineering

Department of Mechanical Engineering, University of Windsor

Submitted on: 2nd August 2023



SAE AERO DESIGN

Ahmedani, Sarmad 110 033 060

Tran, Bryan 104 583 517

Ukiri, Victor 110 015 353

Tuladhar, Riwash 110 011 428

Romanzin, Massimo 105 209 175

Singh, Taman Deep 110 019 465

Mohammed, Ahmad 110 024 613

Faculty of Engineering








Department of Mechanical Engineering, University of Windsor

Submitted on: 2nd August 2023

Signature Page

No action by any design team member contravened the provisions of the Code of Ethics, and we hereby reaffirm that the work presented in this report is solely the effort of the team members and that any work of others that was used during the execution of the design project or is included in the report has been suitably acknowledged through the standard practice of citing references and stating appropriate acknowledgments.

Signature Table

Name	ID Number	Signature	Date of Signing
Sarmad Ahmedani	110 033 060		08/01/2023
Bryan Tran	104 583 517		08/01/2023
Victor Ukiri	110 015 353		08/01/2023
Riwash Tuladhar	110 011 428		08/01/2023
Massimo Romanzin	105 209 175		08/01/2023
Taman Deep Singh	110 019 465		08/01/2023
Ahmad Mohammad	110 024 613		08/01/2023

Abstract

The subsequent report details the Lancer Aerosports team's approach to designing a radio-controlled (RC) aircraft in the Regular Class for the SAE Aero 2023 Competition. The aircraft's primary goal is to carry the maximum feasible weight within specified constraints such as maximum weight, power, and takeoff distance. Additionally, it must be capable of making a turn and returning to the base within a specific time limit. Several challenges related to these constraints have been identified, including a 750W power limit, a runway length of 100 feet, material restrictions like the use of carbon fiber, and wingspan limitations ranging from 120 to 216 inches.

The team's design centers around a 214.66-inch wingspan, employing the Selig S1223 airfoil. The design features a streamlined fuselage to minimize aerodynamic drag, directly transferring all the aerodynamic loading to the wing spars ensuring that the fuselage does not play a crucial structural role.

The payload is securely fastened inside the aircraft's fuselage through a metal bar penetrating all plates. The team opted for balsa wood, spruce wood, pinewood, and aluminum materials to achieve a minimized empty weight while ensuring structural integrity.

To meet the competition's requirements, the team used aerodynamic, structural, and Finite Element Analysis to predict the aircraft's performance up to the desired standard. Various calculations and schematics have been provided as the basis for their predictions of the aircraft's performance and takeoff weight.

A takeoff ground roll of 82 ft, a landing ground roll of 344 ft, and a flight score of 52 is expected to place the team 6th overall for mission scores.

List of Acronyms

C_T ; Coefficient of thrust C_L ; Coefficient of lift C_D ; Coefficient of drag C_P ; Coefficient of Power

FS; Flight Score

PPB; Predicted Payload Bonus

C_{d0} ; Profile Drag

N; Total number of flight rounds during competition, α ; Angle of Attack

ρ ; Density at sea level in imperial units

AR; Aspect Ratio

λ ; Taper Ratio

HT; Horizontal Tail

VT; Vertical Tail

VHT; Horizontal Tail volume, VVT; Vertical Tail Volume, CG; Center of Gravity

M.A.C.; Mean aerodynamic chord ESC; Electronic speed control K_p ; Propeller sizing constant PBHP;

Engine Power (in BHP)

n; Loading factor at a bank angle of 45°

L; Lift force

CNC; Computer Numerical Control

S_g ; Desired takeoff roll distance

AC- Aerodynamic Centre

V_{TO} - Takeoff Velocity

Table of Contents

List of Acronyms	5
List of Tables	9
INTRODUCTION	1
BENCHMARKING	1
Review of Prior Art.....	1
Existing Technologies Review	3
DESIGN CRITERIA, CONSTRAINTS, AND DELIVERABLES	4
Competition.....	4
Constraints	5
Structural constraints	5
Power constraints.....	6
Material Constraints	6
Payload Constraints	6
Mission Constraints	6
Deliverables	6
DESIGN METHODOLOGY	6
Airfoil Selection.....	6
Lifting Surface	7
Wing	7
Horizontal and Vertical Stabilizers.....	7
Control Surfaces.....	7
Aileron	8
Elevator and Rudder	8

Payload Bay	9
Fuselage	10
Aircraft Sectioning.....	10
Landing Gear	12
Nose Gear	12
Main Gear	12
Power	13
Propeller Selection	13
Servos.....	13
Empty Weight Minimization	13
Wing	13
Fuselage	14
Hollowing the airframe.....	14
MODEL IMPLEMENTATION.....	15
MATLAB Math Model.....	15
AVL Model: Flight simulations and Stability	15
CAD Model.....	15
MODEL TESTING/VALIDATION.....	15
MATLAB Math Model.....	16
Aerodynamic Performance analysis (AVL).....	16
Structural Analysis (FEA).....	17
SAE Aero Design West results	19
DESIGN SPECIFICATIONS, PERFORMANCE METRICS	19
Design Specifications.....	19
Power System and Servo Specifications	20

Landing Gear Specifications	21
Fuselage Specifications	21
Design Specifications (Parameters and Values)	21
Score	21
Performance Gap	22
CONCLUSIONS.....	22
REFERENCES	23
APPENDIX A: Take-off and Landing Distance MATLAB Code	24
APPENDIX B: C_l vs α for S123 Airfoil.....	29
APPENDIX C: Geometry File AVL.....	30
Appendix D: Mass File AVL.....	33
Appendix E: Thrust Vs Velocity Graph.....	33

List of Figures

Figure 1: M-14 2022 SAE Aero Design East	2
Figure 2: Competitor I (Apprentice STS)).....	3
Figure 3: Competitor II (Skynetic Trainer King).....	3
Figure 4: Flight Path	4
Figure 5: Historical guidelines for aileron sizing from Raymer (2012)	8
Figure 6: Cargo bay with the hatch closed.....	9
Figure 7: Cargo bay with the hatch open exposing payload plates.....	9
Figure 8: Payload holder	10
Figure 9: Wing sectioning.....	11
Figure 10: Fuselage sectioning	11

Figure 11: Aluminum sleeve connections at wings	11
Figure 12: Steerable Nose gear Strut	12
Figure 13: Commercially available carbon fiber main landing gear	12
Figure 14: Wing ribs	14
Figure 15: Elliptical Cuts in Fuselage Nose cone	14
Figure 16: Fuselage tail boom design	15
Figure 17: Eigenmode Analysis on Athena Vortex Lattice (AVL)	16
Figure 18: Full Aircraft CAD Model	19
Figure 19: Payload Prediction Curve	22
Figure 20: C_l vs α data for s1223 from XFLR5	29
Figure 21: Thrust drop vs Velocity for Small Prop	33
Figure 22: Thrust Drop vs Velocity for Large Prop	34

List of Tables

Table 1: Existing Similar Technologies	3
Table 2: FEA results of wing	17
Table 3: Spar dimensions (in.) based on FEA results	17
Table 4: FEA results for Tail	17
Table 5: FEA results for Payload Bay	18
Table 6: FEA results for Nose Gear	18
Table 7: FEA results for Nose Cone	18
Table 8: Design specifications	19
Table 9: Performance Metrics	21

INTRODUCTION

The 2023 Aero Design Capstone team decided to model the aircraft from the SAE Aero Design Regular Class competition this year, with the challenge to design a remote-controlled (RC) aircraft that could lift off in 100 feet, fly in a circle, then land and stop within 400 feet, all while carrying a payload. The competition design constraints for the aircraft included but were not limited to a minimum of 12 to a maximum of 18 feet wingspan, 750 kW power limiter, and a maximum takeoff weight of 55 lbs. Each part could not be longer than 4 feet, which meant that the team had to design a plane that could be sectioned off and carried by its pieces.

The goal is also to make sure that the plane would be structurally sound, and be able to stay in stable flight, while carrying the payload. Moving forward, the team hopes that the results will bode well with the University of Windsor, the team's sponsor and the team themselves.

BENCHMARKING

Review of Prior Art

In our conceptual design pursuit, an essential step involved initially reviewing the prior research and approaches performed by the previous team to fulfill the problem definition. The mission of the aircraft depends upon the Design Rules set by the 2023 Collegiate Design Series SAE Aero Design Rules, therefore, most of our initial brainstorming came from this document. Every year, the challenge is unique and exciting. The previous year included tennis balls as passengers to simulate airlines, and soccer balls to simulate large cargo, however, this year was different because it was mostly focused on structural efficiency with heavy lifting. Meaning it was to minimize the empty weight of the aircraft as much as possible to increase payload capacity without having any structural disadvantage. This year, the wings were large as the Regular Class was limited to a minimum wingspan of 120 inches. This required removing outer wing panels and a maximum 48 inches measurement of components along the primary axis to ensure smooth movement during the competition. The main challenge was to take off from the runway within 100 feet. Because higher lift generation within a short distance was to be obtained, the initial wing type was chosen to be either Tandem Wing or High Wing. This was because of their high lift generation capability with shorter distances. Due to the complexity of tandem wings, the group decided that the concept of a high wing is much more appropriate. The other challenge was the post-flight activities of unloading the boxed Cargo which had to be completed within a one-minute timeframe. Because the Cargo was unloaded within the time frame and was weighed and recorded for

flight scoring, it was very crucial to us that the design is very simplistic and did not impact the aerodynamical shape. Therefore, that encouraged us to use an upside-down table that has a bay on top to place the payload.

The research was initially conducted on a prior SAE Aero Design Analysis that was created by the University of Michigan. The aircraft they constructed was a high-lift aircraft with a single propeller, capable of carrying a payload of 15 pounds. The aircraft's specifications included an empty weight of 22 lbs., a maximum takeoff weight of 37 lbs., a wingspan of 7.5 ft, and a maximum flight speed of nearly 45 ft/s. This aircraft provided us with a foundational overview of aircraft design and quantified the capability of a high wing from its flight score.



Figure 1: M-14 2022 SAE Aero Design East

Moreover, the SAE Aero Design Project from previous years provided us with methods for approaching similar design challenges. We derived information about diverse materials employed for wings, stabilizers, and fuselages from their project. The consistent similarity between each year's projects was the utilization of the same airfoil profile. Through our Xfoil analysis, we established that Selig 1223 (S1223) was the optimal airfoil for generating high lift at lower Reynold's number and attack of angle. Our comparison with previous reports served to validate our initial assessment, confirming that we were indeed following the correct path.

After having the conceptual design for our aircraft, the preliminary design to quantify various sections of the aircraft was initiated. Each section required intensive numerical and analytical approaches to obtain shape, size, and performance. "Aircraft Design: A Conceptual Approach" by Daniel P. Raymer was a key factor in designing structures, landing gears, and control systems. The study of airfoil selection, wing geometry, and tail arrangement was also performed with it. Example: the main control surface sizing involves dynamic analysis considering structural and control effects. Initial design guidelines suggest aileron area estimation using Figure 5: Historical guidelines for aileron sizing from Raymer (2012). Ailerons usually span about 10-30% of the wingspan. Likewise, a single-engine

propeller was examined using “Thermodynamics and Propulsion” by Prof. Z. S. Spakovszky, Unit: 11.7 Performance of Propellers. It helped us calculate the mathematical expressions governing thrust, torque, and propulsive efficiency for the propeller. Following the sizing of each section, we established a system to assess aircraft stability in AVL software. After that, each section was subdivided for detailed analysis—e.g., wings into spars, ribs, and skin. We utilized MATLAB for flight calculations and SolidWorks/CatiaV5 for structural evaluation.

Existing Technologies Review

We examined various single-propeller and high-wing aircraft designs present in the current market. Analyzing these contemporary designs gave us insight into the features utilized by the current market. This process aided us in comprehending the importance of specific design specifications, including control surfaces, servos, landing gear configurations, and more.

Table 1: Existing Similar Technologies



No.	Competitor Name	Features	Appearance
1	Apprentice STS 1.5m RTF Basic Smart Trainer with SAFE	<ul style="list-style-type: none"> • Power Type – Electric • Material - EPO • Wingspan - 59.02 inches • Brushless Outrunner Motor • No Flaps • 37g Servo • Landing Assist Sensor • Technology - Smart, AS3X, and SAFE 	
2	Skynetic Trainer King	<ul style="list-style-type: none"> • Landing Gear - Tri-gear Fixed. • Wingspan 44.0 inches • 4x 8g servos • Control Surfaces - All • No Flaps • Hinge Type Foam Material EPP Foam 	

Figure 2: Competitor I (Apprentice STS))

Figure 3: Competitor II (Skynetic Trainer King)

DESIGN CRITERIA, CONSTRAINTS, AND DELIVERABLES

The design criteria used to optimize the design and on which design decisions are based, the constraints that limit design decisions, and the final design deliverables are provided and discussed.

Competition

The basis for major design choices is the SAE Aero Design West scoring equation:

Equation 1: Scoring Equation

$$FFS = \text{Final Flight Score} = FS_1 + FS_2 + FS_3 + WS$$

$$FS = \text{Flight Score} = \frac{W_{\text{payload}}}{2} + PBB$$

$$PBB = \text{Payload Prediction Bonus} = \text{MAX}(5 - W_{\text{payload}} - P)^2, 0)$$

$$WS = \text{Wingspan Score} = 2^{(1+\frac{b}{5})}$$

$$W_{\text{payload}} = \text{Regular Boxed Cargo Weight(lbs)};$$

$$b = \text{Aircraft Wingspan(ft)}; P = \text{Predicted Payload}$$

Flight mission:

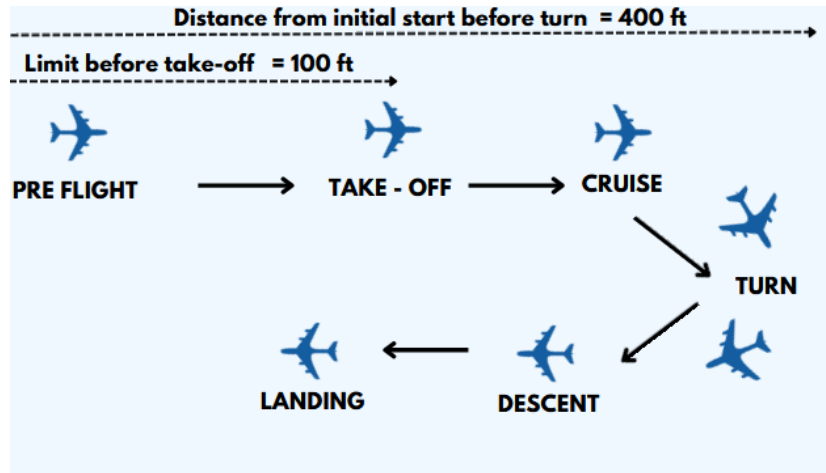


Figure 4: Flight Path

Looking at Equation 1: Scoring Equation, the two major parts constituting the equation are the three-flight score and the wingspan.

Flight Score

Flight Score evaluates the team's ability to correctly predict the payload capacity in the design phase and the aircraft's ability to perform the required maneuvers 3 times. The three flight scores are then added together. The flight path is given in Figure 4: Flight Path. The flight path includes a limited

runway with a takeoff phase followed by a climb, cruise, turn, descent, and land phase. The flight path is distance and time-limited, which will be discussed later.

Taking apart the flight score formula, it can be observed that part of the score is based on the Payload Prediction Bonus which accounts for the difference between the predicted (design) payload and the actual weighted payload. The predicted payload is determined from the payload predictive curve. With no difference, 5 points would be the maximum awarded which would mean that the team accurately predicted the payload capacity and received 100% of the points. This bonus is then added to half the actual weight of the payload. This means that an increase of a minimum of 10 lbs. in the actual weight of the payload would be needed to offset a difference of 3 lbs. (which would result in a zero PPB).

Wingspan Score

Having Wingspan in the scoring equation dictates that if other factors are ignored, the increase in wingspan would increase the score. If parameters such as empty weight, payload capacity, ground roll, and flight stability are considered, then maximizing the score depends on the trade-offs that exist between contradicting parameters. Since the wingspan is constrained to 18 ft., a maximum of 24 points can be achieved with this wingspan.

Constraints

SAE Aero Regular Class competition offers various constraints that have a major impact on aircraft design and manufacturing.

Structural constraints

Arguably, the most important dimensional constraint. With a maximum wingspan of 18ft and a minimum wingspan of 120 in, there is a very high potential for the wingspan to be utilized to gain a high score at the competition considering that Equation 1: Scoring Equation favors a wider wingspan over a narrower one. This would result in reduced structural support required from other parts of the aircraft adding to the payload capacity.

In addition, no part of the aircraft should exceed a total length of 4 ft. This major constraint thus requires that the aircraft be designed in sections that pose more design challenges and obstacles. Lastly, the minimum wingtip cord is 4 in. It is also important that the outer sections of the aircraft be removable.

Finally, the aircraft may not weigh more than 55 lbs. This means that the focus will be on reducing empty weight and increasing payload capacity.

Power constraints.

The aircraft must be powered by a 6-cell (22.2volt) Lithium-Polymer battery pack. Minimum requirements: 3000 mAh, 25c attached to a motor that rotates the propeller. The motor is also connected to a 1hp. power limiter. A one-to-one RPM between the propeller and motor must be maintained.

Material Constraints

No part of the aircraft should have Fiber- Reinforced Plastic (FRP) including duct tape. Exceptions include commercially available FRP motor mount, propeller, landing gear, and control linkage components.

Payload Constraints

The payload must consist of regular boxed cargo and access to the cargo must be easy. This is because the unloading phase of the payload is time restricted to a maximum of 1 minute and 2 members are allowed to participate. The cargo bay has no geometric or dimensional restriction though it may not be exposed to the stream of air at any time. A metal bar must penetrate the payload plates through the fuselage.

Mission Constraints

A successful flight attempt requires that the wings are successfully assembled at the race line, followed by a ground roll limit of 100 ft. meaning that the aircraft must take off before this distance is covered. The aircraft then must at least travel 400ft. before making a turn and returning to land within 400 ft. of the landing runway.

Deliverables

The most important project deliverable is achieving a high score at the SAE Aero Design Competition with a RC aircraft designed to maximize wingspan and payload capacity. In addition, it's also important that research and knowledge on the project be shared with the next team as part of the improvement in performance at the SAE Aero Design Competition 2024 and education.

DESIGN METHODOLOGY

Airfoil Selection

Selig 1223 (S1223) is the airfoil section the aircraft would utilize as it is a low Reynolds number high lift airfoil. Its large lift-to-drag ratio is crucial to ensure a maximized payload carrying capacity, necessary to achieve high flight scores.

Lifting Surface

Wing

The three major factors that influence the design of the wings are Aerodynamics, takeoff ground roll distance, and the flight scoring formula. It is essential to design a wing with high aerodynamic efficiency, as it would improve the overall lifting capacity of the aircraft. The wing must also provide the required lift to take off within the 100ft ground roll when empty and when loaded with payload. Lastly, as the aim is to achieve a high wingspan score, maximizing the wingspan within reasonable limits helps achieve this. The larger wingspan aids in improving the aerodynamic performance of the wing as we achieve an aspect ratio of 10 while ensuring the wing reference area of 32 ft² is sufficient for takeoff roll.

$$V_{TO} = [2 * W / (S_{ref} * r * 0.8 * C_{Lmax})]^{0.5}$$

Equation 2: Required Takeoff velocity.

$$a = \left(\frac{g}{W}\right) * [(T - D) - F_C * (W - L)]$$

Equation 3: Takeoff Acceleration

$$S_g = V_{TO}^2 / 2 * a_{mean}$$

Equation 4: Takeoff ground roll distance

As a justification for wanting a high reference area of 32 ft², we observe equations 1 and 3 courtesy of Nicolai (2002) we see the importance of increasing the reference area S_{ref} to reduce required takeoff velocity in turn shortening takeoff ground roll.

Horizontal and Vertical Stabilizers

The horizontal and vertical are sized using the tail volume coefficient method proposed by Nicolai & Carichner (2010). For general aviation aircraft, it suggests a CHT of 0.7 and CVT of 0.032 for single propeller engine aircraft. The tail arm of the stabilizers is 60 percent of the fuselage length as suggested by Raymer (2012) for front-mounted propeller aircraft.

Control Surfaces

Designing the control surfaces to guarantee authority and reliability in flight aids the overall success of an aircraft's mission. Raymer (2012) provides excellent insight into the sizes of control surfaces based on the percentage chord and percentage span of their respective components, wings, horizontal stabilizer, and vertical stabilizer.

Aileron

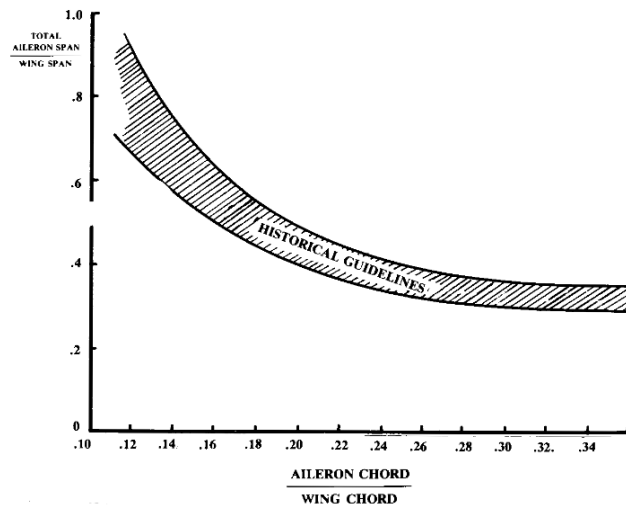


Figure 5: Historical guidelines for aileron sizing from Raymer (2012)

Taking insights from Raymer (2012), the team sized the aileron to ensure adequate bank capacity and hinged it at 75 percent of the wing chord, spanning 35% of the wingspan.

Elevator and Rudder

To achieve reliable elevator control, hinge it at 65 percent chord, spanning 100 percent of the horizontal stabilizer wingspan. For Rudder authority, we utilize the same approach hinging it at 65 percent chord and spanning 100 percent of the horizontal stabilizer.

Payload Bay

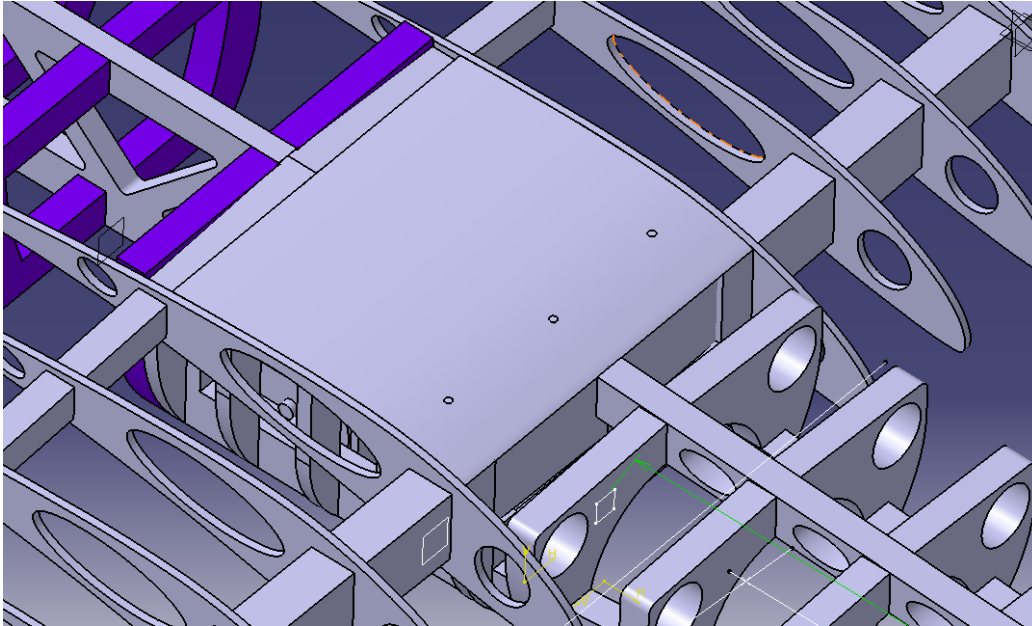


Figure 6: Cargo bay with the hatch closed

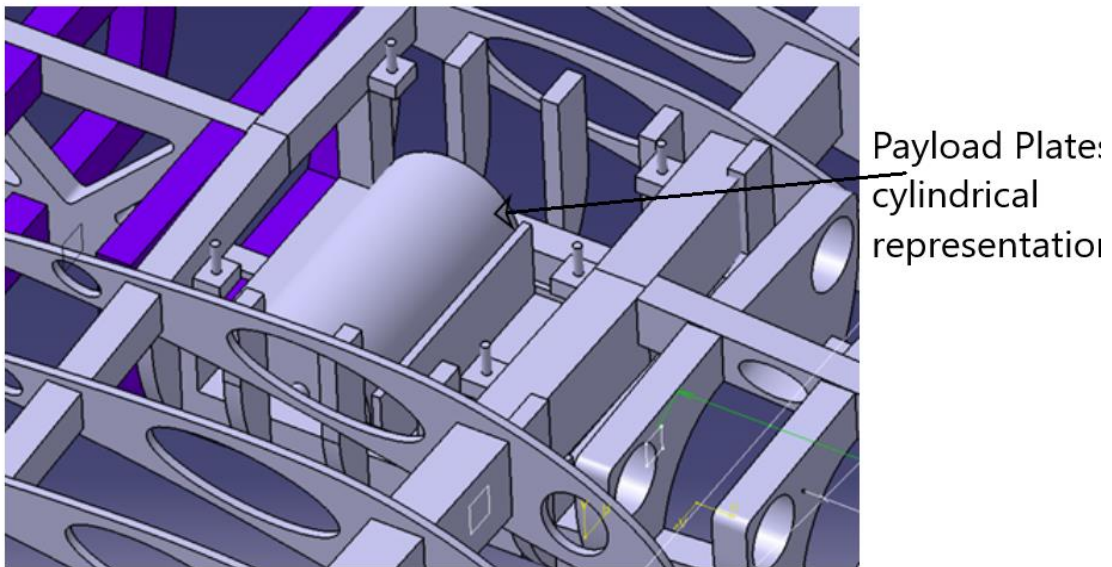


Figure 7: Cargo bay with the hatch open exposing payload plates

The SAE Aero design competitions rules require the payload bay to be fully enclosed and unexposed to airflow. A metal bar must also penetrate each plate. Considering these constraints along with prioritizing quick access to the payload plates leads to the adoption of a top hatch in the aircraft which is screwed on and off for access.

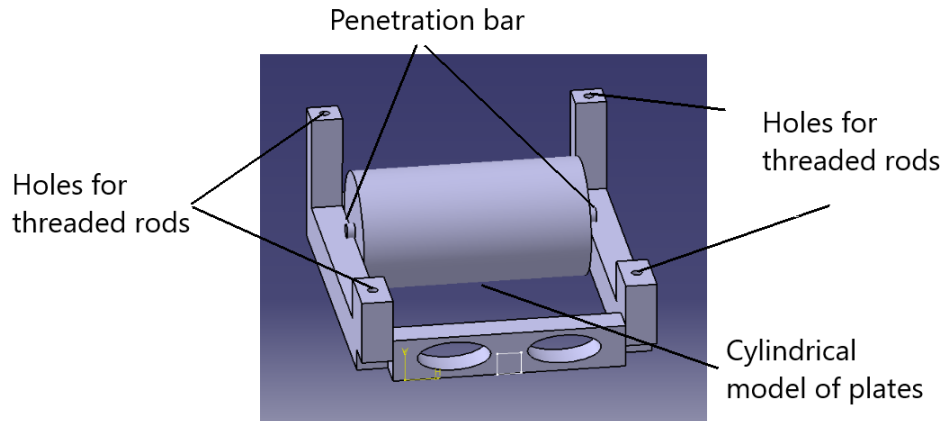


Figure 8: Payload holder

As we prioritize transferring all the loads directly to the wing spars, an “upside-down table” payload holder is utilized. Connecting to both the aft and main wing spars of the aircraft through embedded threaded rods and washers.

This payload holder also acts as a direct transfer of load from the wings to the landing gear upon landing.

Fuselage

The approach to designing a fuselage was for it to act as an aerodynamic bag. It is to have no significant mass of its own and its only purpose is to make the overall design aerodynamic. The material used for the fuselage will be XPS foam and Monokote wrapping.

Aircraft Sectioning

To adhere to the SAE Aero design west 2023-competition constraints a modular approach is used to design the aircraft ensuring no individual component is more than 4ft in any primary axis. Dividing the wing into 5 sections and the fuselage into 3 satisfies the constraint.

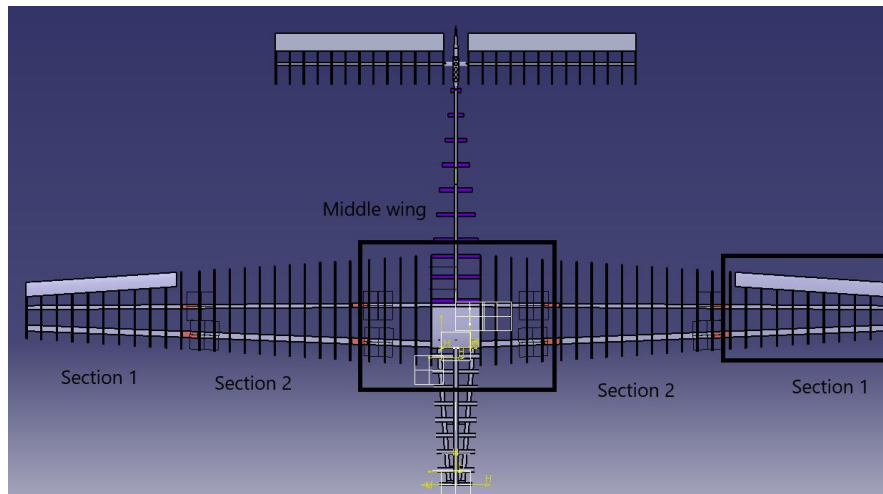


Figure 9: Wing sectioning

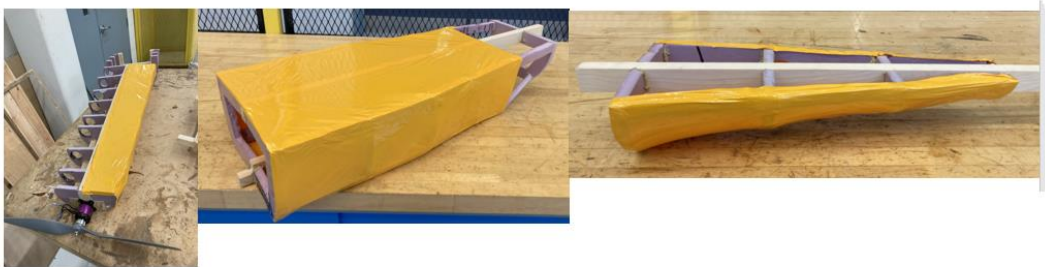


Figure 10: Fuselage sectioning

To connect the separate components, high-strength Aluminum sleeves, and bolts secure wing sections together at the spars. In figure 11, the sleeves are pink to differentiate from the wooden components.

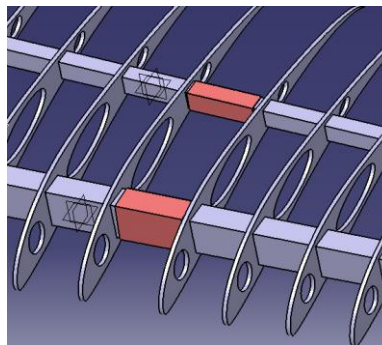


Figure 11: Aluminum sleeve connections at wings

The fuselage uses the same approach as figure 11 to connect both sections of the tail boom. For the connection of the fuselage to the payload bay and nose cone section. A threaded rod, nut, and bolts secure the parts together.

Landing Gear

The final design utilizes tricycle landing gear cause of the steering requirements and ease of manufacturing. The weight distribution for the nose gear and main gear was 6% and 94% respectively.

Nose Gear



Figure 12: Steerable Nose gear Strut

It is important to ensure the aircraft is steerable while on the ground as relying on the control surfaces at slow taxi speeds for steering is inadequate. Selecting steel as the desired material ensured excellent fatigue strength. A Robart steerable fixed nose gear strut able to support aircraft up to 50 lb along with a 4-inch diameter wheel satisfies the necessary loading requirements of the nose gear.

Main Gear



Figure 13: Commercially available carbon fiber main landing gear

A commercially available carbon fiber-reinforced plastic main landing provides excellent fatigue resistance while being extremely lightweight. The landing gear is for aircraft up to 55 lb; through testing, we observed it supports compressive loads in excess of 100 pounds.

Power

The heart of the airplane is an HRB 6S 22.2V 5000mAh LiPo battery. It is the most important piece of the airplane because it powers all the servos and electronics on the aircraft. It will be powered by a Hacker A50-16L V4 brushless motor. With the constraints on the power available, it was crucial to maximize the thrust we could generate.

Propeller Selection

Equation 2 portrays the importance of increasing the thrust in reducing the takeoff ground roll distance. The takeoff acceleration depends heavily on static thrust, increase in thrust, increase in acceleration, and decrease in takeoff ground roll. Due to the power limit, it is important to maximize the thrust available for the takeoff roll; the propeller selection directly influences this.

Raymer (2012) presents an equation directly relating propeller diameter to Hp available. For a two-blade propeller, the equation

$$d = 22\sqrt[4]{Hp}$$

Equation 5: Propeller diameter as a function of Horsepower

With d representing propeller diameter and Hp representing available horsepower. At 1 hp this gives us a diameter of 22 inches. Knowing the required propeller diameter to utilize the max Hp we utilize an APC 22x12 WE propeller.

Servos

There are six servos within the aircraft. One for each aileron on each side of the wings, one for the elevator, one for the rudder, and another for the nose gear.

Empty Weight Minimization

Minimizing the empty weight of the aircraft is crucial to increasing the payload-carrying capacity of the aircraft. Material selection and structural design methodology are crucial to reducing empty weight.

Wing

Regarding material selection for the wings, we focus on selecting materials with excellent strength-to-weight ratios. Balsa wood is a widely used material for the ribs of wings with the team utilizing Spruce wood for the spars.

The structural design of the wing spars and ribs aids in further reducing the empty weight. The spar is a hollow box beam while the addition of multiple circular and elliptical cuts to the ribs reduces the collective weight of the ribs.

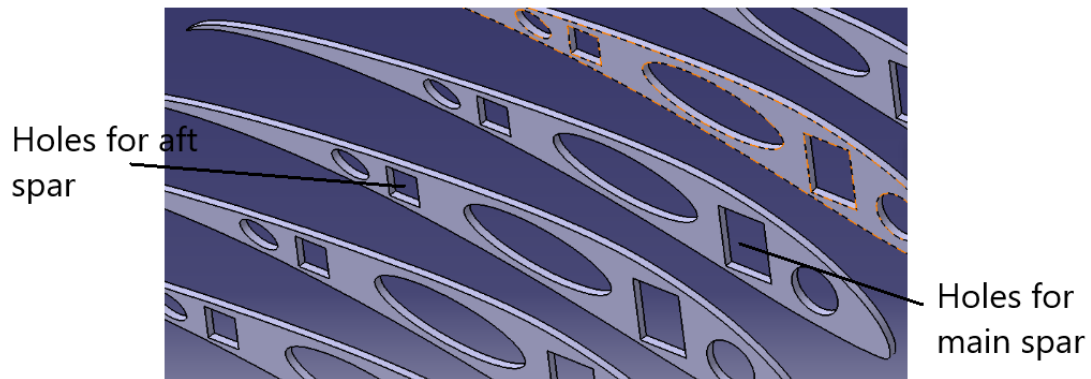


Figure 14: Wing ribs

Fuselage

The approach to designing the fuselage as a bag for the payload bay meant exploring ways to minimize structural support through the fuselage. We approached this by eliminating the use of a fuselage spar as a central hub to transfer all the aircraft loads. Transferring all the loads to the wings instead significantly minimized the empty weight of the aircraft.

Hollowing the airframe

Incorporating multiple holes into the airframe's structure in positions that do not compromise structural integrity minimizes the overall empty weight of the aircraft.

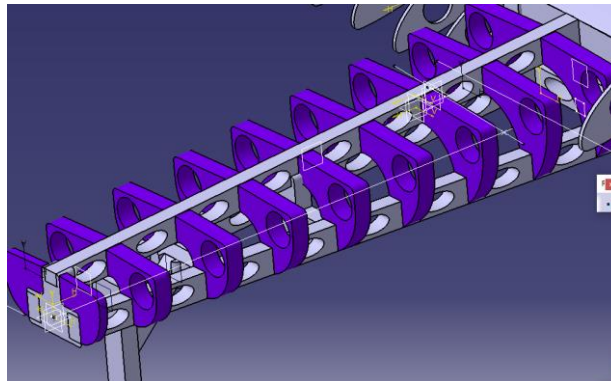


Figure 15: Elliptical Cuts in Fuselage Nose cone

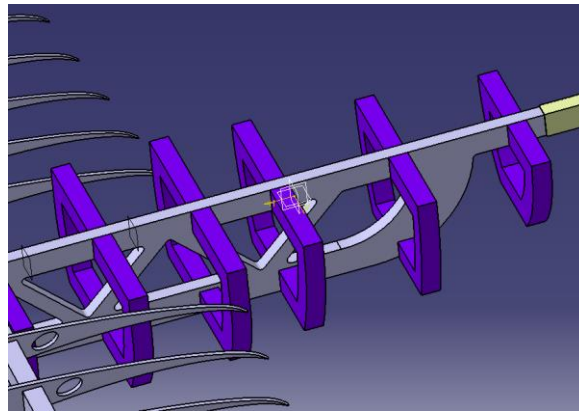


Figure 16: Fuselage tail boom design

MODEL IMPLEMENTATION

MATLAB Math Model

The takeoff ground roll was modeled using a MATLAB script that first determined the required takeoff velocity and then calculated the mean acceleration at 70.7% of V_{TO} . With the information available from the propeller vendor charts the dynamic thrust at 70.7% was determined and used in the calculations.

AVL Model: Flight simulations and Stability

To ensure dynamic and static stability in all flight modes AVL's Eigen mode analysis is utilized. The geometry file of the aircraft considering the dimensions and positions of all the aircrafts components. A mass distribution file is developed in conjunction with the geometry file and a run case file is developed to execute the operation at the desired phases of flight. Meeting the criteria for static stability during all phases of flight, the aircraft requires the CG to be between the AC and the neutral point. After confirming the static stability criterion, the dynamic stability of the aircraft was analyzed. To be dynamically stable the aircraft must show a tendency to correct itself to its trim state after a perturbation.

CAD Model

Knowing the dimensions of each aircraft subsystem, a CAD model of the aircraft was developed utilizing CATIA V5. This model improved the accuracy of the CG estimation enabling us to perform iterative analysis on the stability of the aircraft improving the results of our Eigenmode plots.

MODEL TESTING/VALIDATION

Model testing and validation conducted on various aspects of the airplane typically referring to the process of ensuring the safety, performance, and compliance of an aircraft's design and systems.

MATLAB Math Model

Using a MATLAB script that utilized equations 2, 3 and 4 to compute the required takeoff velocity, mean acceleration at 70.7% of VTO, and takeoff ground roll, we analyze the model at the empty weight of the aircraft, which changes iteratively. An empty weight that met the takeoff ground roll requirement is 22 lbs.

Aerodynamic Performance analysis (AVL)

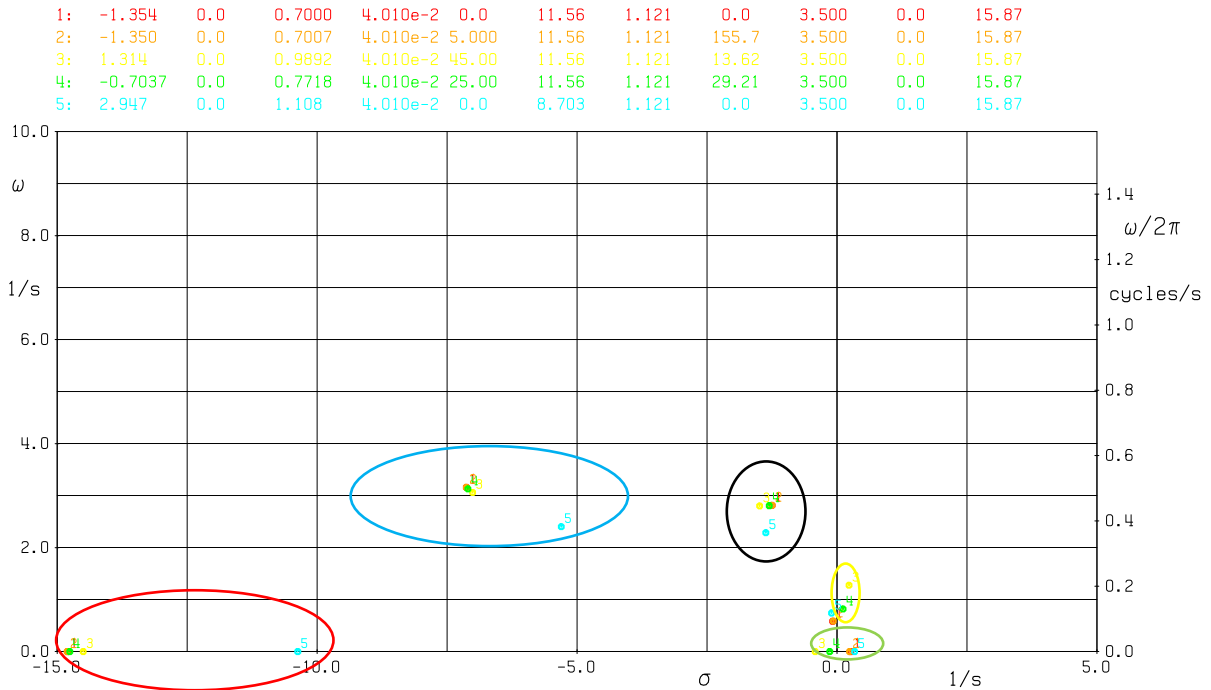


Figure 17: Eigenmode Analysis on Athena Vortex Lattice (AVL)

Red represented Roll subsidence, blue represents a short period, black represented Dutch roll, yellow represents Phugoid, and green represented Spiral. The aircraft was stable in all modes except Spiral mode and Phugoid mode. In spiral mode, it was critically un-damped and unstable, but it took a long-time post perturbation for the aircraft to lose control. The real sigma values were also much less than 1 for all flight phases, which reassured adequate time to control the unstable spiral. The Phugoid mode was stable for climb and cruise, but for bank angles greater than 5° , it was unstable. To address the unstable Phugoid modes during banking maneuvers, we ensured the real values of the modes were <1 , and the time period with the unstable modes was much larger than the time it took to perform the turns. After confirming this in the Eigenmode animation, we were confident that the aircraft would not go out of control during a bank and met the dynamic stability criterion for all other phases of flight.

Structural Analysis (FEA)

The Finite Element Method is utilized on many parts of the plane to validate their required strength. The cantilever deflection under a distributed load was employed to analyze the structural integrity of the wing design. The deflection helped in determining the second moment of inertia of the beam, which, in turn, was utilized to find the dimensions of the cross-section. To verify the results of the numerical analysis, Finite Element Analysis (FEA) was employed multiple times on the wing design. Loads were applied using an elliptical distribution along the span of the wing during these analyses. The table below shows the constraints and FEA results.

Table 2: FEA results of wing

Parameters/ Constraints	Values	FEA Results (Wing)	Values
Maximum allowable bending stress	3300 psi	Maximum bending stress	3280 psi
Max allowable deflection	7.50 in	Max deflection	6.92 in

The FEA results depict the values within the constraints. Below are the spars dimensions devised from the analysis:

Table 3: Spar dimensions (in.) based on FEA results

Main Spar Dimensions		Second Spar Dimensions	
Root	2.45 x 1 in	Root	1.25 x 1 in
Tip	1.5 x 1 in	Tip	0.5 x 1 in
Thickness	0.2 in	Thickness	0.2 in

Similarly, again the transitional loadings were applied on the tail of the airplane, tables below show the FEA results and dimensions validated for the tail spars and length.

Table 4: FEA results for Tail

FEA Results (Tail)	Values	Name	Dimensions	Length	Material
Maximum bending stress	742 psi	Vertical Stabilizers Spar	0.75 x 0.75 in	27.17in	Spruce wood
Max deflection	1.39 in	Horizontal Stabilizer Spar	1 x 1 in	90.12	Spruce wood

Length of Tail boom	2 x 1 in	46.96 in	Spruce wood
---------------------	----------	----------	-------------

Table 5: FEA results for Payload Bay

FEA Results (Payload Bay)	Values	Material
Maximum bending stress	2465.64 psi	Pinewood
Max deflection	0.06 in	Pinewood

To assess the payload holder's capacity to withstand the weight of the payload, a load equivalent to three times the payload weight was applied, and Finite Element Analysis (FEA) was performed. The analysis results showed that the maximum bending stress reached was 2465.64 psi, which was lower than the calculated yield stress of the Pine, around 6000 psi. This indicated that the payload holder can endure three times the weight of the payload without experiencing significant deflection.

Table 6: FEA results for Nose Gear

FEA Results (Nose Gear)	Values	Material
Maximum bending stress	232.06 psi	Aluminum
Max deflection	0.03 in	Aluminum

To assess the nose gear's ability to withstand the motor's thrust and the applied weight, a Finite Element Analysis (FEA) was conducted. The analysis showed that the maximum bending stress reached was 232.06 psi, which is lower than the calculated yield stress of the material. This indicates that the nose gear can effectively handle both the thrust force from the motor and the weight force applied to it. Similarly, the same analysis was used to validate nose cones.

Table 7: FEA results for Nose Cone

FEA Results (Nose Cone)	Values	Material
Maximum bending stress	535 psi	Pinewood
Max deflection	0.0376 in	Pinewood

DESIGN SPECIFICATIONS, PERFORMANCE METRICS

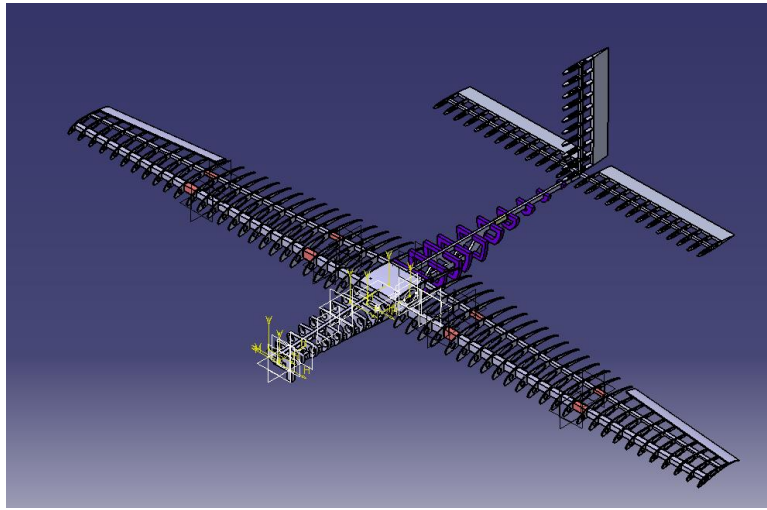


Figure 18: Full Aircraft CAD Model

Design Specifications

After going through optimization, modeling, and validation, the final design of the aircraft was settled upon by the team. The most important key design specifications are shown in Table 8. In the project documentation, individual parts and assemblies with their detailed specifications and drawings are presented.

Table 8: Design specifications

Design Specification	Value
Lifting & Control Surfaces:	
Wing Airfoil	Selig 1223 (S1223)
Wingspan	17.888 ft
Aspect Ratio	10
Wing Chord	2.317 ft
Wing Anhedral	2°
Wing Mean Chord	1.856 ft
Horizontal Tail Area	8.057 ft ²
Vertical Tail Area	3.551 ft ²
Reference Area for Wing @ Aspect Ratio (10)	32 ft ²

Overall Aircraft Length	9.5 ft
Power System & Servos:	
Motor Power	750 W
Battery Capacity	5000 mAh
Propellor	APC 22x12WE
Servo	d SAVÖX SC-1251MG
Landing Gear:	
Configuration	Tricycle – 1 Nose Wheel, 2 Main Wheels
Fuselage:	
Cargo Bay Length	0.78 ft
Cargo Bay Height	0.37 ft

One of the most fundamental aspects of the aircraft is the Selig-1223 airfoil. It is very commonly used in the SAE Aero design competition because of how it provides excellent lift capabilities at lower Reynolds numbers. While the aircraft's maximum allowable wingspan is 18 ft decided on by the competition rules, a wingspan of 17.888 ft was chosen. This is because a highly efficient wing design is crucial for improved lift capacity. Added stability is provided to the aircraft by the 2° wing dihedral. The vertical and horizontal tail areas, as well as the overall length of the aircraft are designed to ensure ample control over the elevator and rudder functions. This generates significant pitch and yaw moments around the aircraft's center of gravity.

As for the materials of the components of the aircraft, the ribs are made from balsa wood, the spars are pine, and the leading and trailing edges are extruded polystyrene (XPS) foam. The reasoning behind this selection was to use pine in the highly loaded areas, balsa in areas that are moderately loaded, and XPS in areas that have low loading.

Power System and Servo Specifications

The aircraft is powered by a 750 W brushless DC motor, which was limited by the competition rules. The team chose APC 22x12WE as their propeller due to its capability to maximize thrust through a large diameter and high pitch. Regarding the battery, the team opted for the HRB 6S 22.2V 5000 mAh LiPo due to its capacity to provide sufficient time for the aircraft to complete the circuit and its weight being light. Servos were used for controlling the control surfaces and the landing gear to provide precise and responsive control of the aircraft.

Landing Gear Specifications

The tricycle landing gear configuration was chosen for this aircraft for its simplicity and functionality. It provides the aircraft with higher stability, can handle the steering requirements for the aircraft and is easier to manufacture. Steel was chosen as the material for the landing gear because of its exceptional fatigue strength. A Robart steerable fixed nose gear strut that can accommodate the aircraft weighing up to 50 pounds was used. Additionally, the diameter of the wheel is 4 inches. These all help fulfil the essential load criteria for the nose gear.

Fuselage Specifications

The fuselage has a width of 12 inches and a length of 9 inches. These dimensions were chosen to accommodate enough room for the projected payload of the aircraft.

Design Specifications (Parameters and Values)

Modelling and simulation can predict the performance specification metrics based on the aircrafts design. This is shown in Table 9.

Table 9: Performance Metrics

Performance Specification	Value
Flight Score	52
Takeoff Speed	26.382 ft/s
Cruise Speed	38 ft/s
Cruise L/D	12 ft/s
Empty Weight	18.7 lb
Takeoff Weight	35 lb

The takeoff speed and the cruise speed have a difference of 11.618 feet per second. Since it is not required for the aircraft to complete the circuit within a specified time limit, there is no advantage of having cruise speed much faster than the takeoff speed. Furthermore, having a low cruise L/D for the aircraft is also due to the competition rules and has no noticeable advantage to cruising efficiently.

Score

SAE Aero Design West Scoring equation (Equation 1) was used to calculate the flight score, payloads weight and was used for the basis for the major design of the aircraft. As shown in Figure 19, The density altitude decreases as the payloads weight increases. The payload's weight was found to be 14.836 pounds. This is due to the limitation of having the aircraft flying no higher than 75 feet.

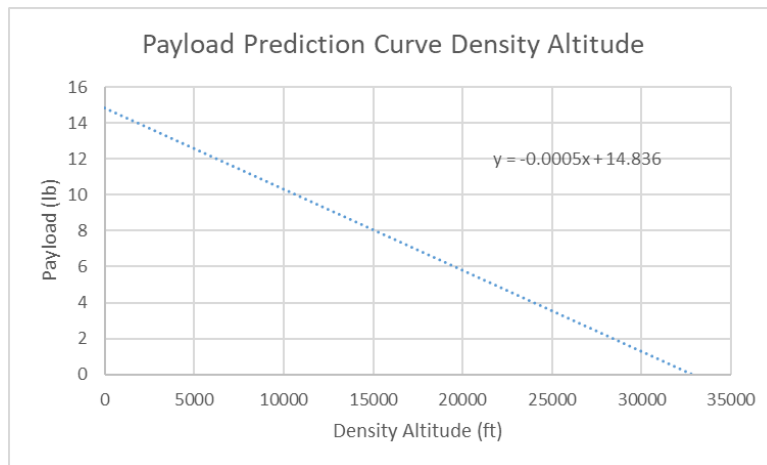


Figure 19: Payload Prediction Curve

Performance Gap

It can be noted that the design score and the flight score that were achieved for the report would have placed us in 6th place relative to the SAE Aero Design West competition, but the team ran into some issues when submitting. Due to the issues, a design score of 43 points was achieved. As for the flight score, 52 points were achieved in total.

CONCLUSIONS

This year's SAE Aero Design team designed an airplane that has a wingspan of almost 17.9 feet, and a length from nose to tail of 9.5 feet. The aircraft would be able to carry about 14.8 lbs., which would make the predicted flight score of the team's aircraft performance at 52 points. That would place their aircraft 6th overall out of the competition held in Texas.

Using inspiration from past teams' design, the S1223 airfoil was used. AVL and FEA analysis helped determine the stability and structure of the plane, respectively. Once it was determined that the airplane could fly, the team moved forward into the manufacturing phase.

However, due to the poor time management, the team could not finish building the aircraft in time. Future advice for the future teams is to start the manufacturing phase as soon as possible, to allow time for materials to come through, but also to allow enough time to adapt for any obstacles that can come along the way, such as broken parts or critical error in design.

REFERENCES

Apprentice STS 1.5m RTF Smart Trainer with SAFE. (n.d.). Retrieved from Horizon Hobby:

<https://www.horizonhobby.com/product/apprentice-sts-1.5m-rtf-smart-trainer-with-safe/EFL3700.html>

Manufacturing, R. (2014). Retrieved from RoboStruts>Nose Gear-Robert Manufacturing:

<https://robart.com/collections/robostruts-nose-gear>

Propellers, A. (2023). Retrieved from Engineering - APC Propellers: www.apcprop.com/technical-information/engineering

Gudmundsson, S. (2013). *General aviation aircraft design: Applied Methods and Procedures*. Butterworth-Heinemann.

Nicolai, L. M., & Carichner, G. E. (2010). *Fundamentals of aircraft and airship design: Volume I—aircraft design*. American Institute of Aeronautics and Astronautics, Inc.

Propellers, A. (2023). Retrieved from Engineering - APC Propellers: www.apcprop.com/technical-information/engineering

Raymer, D. (2012). *Aircraft design: a conceptual approach*. American Institute of Aeronautics and Astronautics, Inc.

Manufacturing, R. (2014). Retrieved from RoboStruts>Nose Gear-Robert Manufacturing:

<https://robart.com/collections/robostruts-nose-gear>

APPENDIX A: Take-off and Landing Distance MATLAB Code

```
% optimal fuselage length
clear;clc;
w0= 35;

%Historical values for a and c
a=3.68;
c=0.23;

%Fuselage length formula
%f_length=a*w0^c;
f_length=8.5965;

%fprintf('Fuselage length is %f ft\n',f_length) %length display change in ft

%flight velocity (keep constant when you want to see how FL affects drag
%on stabilizers)
CL_max=2.025; %airfoil dependent from excel file
%i=20;
rho=0.0023769;
mu=3.677*10^(-7);
ar_w=10;

wings = [];
flightscore = [];
emptyw = [];
a= zeros([1 7]);
for i = 25:1:32
    wingsp = ((i*ar_w)^0.5);
    disp(wingsp)
    fv=1.2*(2*w0/((i)*rho*0.8*CL_max))^(0.5); %Factor in 1.2 from airship design
    %fv=40;
    q=0.5*rho*(fv^2); %dynamic pressureFrom fundamentals of airship design page 73

%fprintf('Take-off velocity is %f ft/s\n',fv)

%Drag portion

%fuselage drag
%d_fuse=0.33333*f_length; %FR assumed to be 3
d_fuse=1;
%d_fuse=f_length/3;
Sref_fuse=6.816; %Reference area of fuselage calculated from planform
Swet_fuse=28;
FR=f_length/d_fuse; %Fineness ratio
%FR=3;
FFf=1+(60/((FR)^(3)))+0.0025*FR; %Form factor
re_fuse=rho*f_v*(f_length/mu); %Fuselage reynolds number
cft_fuse=0.074/((re_fuse)^(0.2)); %Skin friction of fuselage
Cdmin_fuse=FFf*cft_fuse*Swet_fuse/i;
%fprintf('cdmin fuse is %f\n',Cdmin_fuse)

%Wing drag
```

```

tr_w=0.5; %Taper ratio
bw_w=(ar_w*(i))^0.5; %Wingspan based on constant aspect ratio and wingarea
%disp(bw_w)
%disp(bw_w)
Swet_wing=2*i; %Double the reference wing area
cr_w=(2*i/bw_w)/(1+tr_w); %root chord wing
mac_w=(2/3)*cr_w*((1+tr_w+tr_w^2)/(1+tr_w)); %Mac wing
t_c=0.121; % Airfoil dependent
FFw=(1+2*(t_c)+100*((t_c)^4))*1.05; %Form factor of wing check for Airfoil dependence
re_w=rho*f_v*mac_w/mu; %Reynolds number of wing based on chord
%disp(re_w)
% Add laminar cft
cft_wing=0.074/(re_w^0.2); %Turbulent skin friction wing (check for turbulence)
Cdmin_wing=FFw*cft_wing*Swet_wing/i;
%fprintf('Cdmin wing %f\n',Cdmin_wing)

%Horizontal stabilizer drag

ar_h=7; %Aspect ratio
tr_h=1; %Taper ratio
cht=0.7; %Volume coefficient
lht=0.6*f_length; %Tail arm
Sht=cht*mac_w*i/lht; %Reference area
Swet_h=2*Sht;
bw_h=(ar_h*(Sht))^0.5;
%cr_h=(2*Sht/bw_h)/(1+tr_h); %root chord horizontal stabilizer
cr_h=bw_h/ar_h;
%disp(cr_h)
mac_h=(2/3)*cr_h*((1+tr_h+tr_h^2)/(1+tr_h)); %Mac wing
t_ch=0.09; % Airfoil
FFh=(1+1.2*(t_ch)+100*((t_ch)^4))*1.05; %Form factor
re_h=rho*f_v*mac_h/mu; %Reynolds number of wing
%disp(re_h)
cfl_h=1.328/(re_h^0.5); %laminar
Cdmin_h=FFh*cfl_h*Swet_h/Sht;
%fprintf('Cdmin h %f\n',Cdmin_h)

% Vertical Stabilizer drag

ar_v=2; % Vertical tail aspect ratio
tr_v=1; %Taper ratio
cvt=0.032; %Tail volume coefficient
lvt=lht; %Tail arm
Svt=cvt*bw_w*i/lvt; %Reference area
Swet_v=2*Svt; %Wetted area
bw_v=(ar_v*(Svt))^0.5; %Wing span
%cr_v=(2*Svt/bw_v)/(1+tr_v); %root chord horizontal stabilizer
cr_v=bw_v/ar_v;
%disp(cr_v)
mac_v=(2/3)*cr_v*((1+tr_v+tr_v^2)/(1+tr_v)); %Mac wing
t_cv=0.09; % Airfoil dependent tc ratio
FFv=(1+1.2*(t_cv)+100*((t_cv)^4))*1.05; %Some airfoil dependent values are present
re_v=rho*f_v*mac_v/mu; %Stabilizer Reynolds number
%disp(re_v)
cfl_v=1.328/(re_v^0.5); %laminar
Cdmin_v=FFv*cfl_v*Swet_v/Svt;
%fprintf('Cdmin v %f\n',Cdmin_v)

```

```

%Landing gear drag
Cd_gear=1.01; %single strut based off white paper reference 3
g_area=(1.76*4.15)/(12^2); %Frontal area of landing gear
Cadmin_gear=(3*1.01*g_area)/(i);

%Engine drag
cd_engine=0.25; %from white paper, for cowled engine
e_area=22*1.38/144; %frontal area of engine based on propeller area, hud diameter of 1.38 in, prop diameter of 22
cdmin_engine=cd_engine*e_area/i;

%Total Cadmin
Cadmin_total=Cadmin_fuse+Cadmin_wing+Cadmin_h+Cadmin_v+Cadmin_gear+cdmin_engine;
%fprintf('Total Cadmin is %f\n',Cadmin_total)

%Complete drag equation

%Oswald efficiency factor
e0=1.78*(1-0.045*(ar_w^0.68))-0.64;
K=1/(pi()*ar_w*e0); %Induced drag factor utilizing oswald efficiency factor

g=32.22; %acceleration due to gravity in imperial units
KK=0.0172; %from airfoil excel graph
CL=0.7; %airfoil dependent correct for 3d finite;
Cl_min=1.2382; %airfoil dependent
CLg=0.7; %3d wing dependent

CD=Cadmin_total+(K*(CL^2))+KK*(CL-Cl_min)^2; %not yet added landing gear effect
CDg=Cadmin_total+(K*(CLg^2))+KK*(CLg-Cl_min)^2; % CD during ground roll
% AIRCRAFT PERFORMANCE (Level unaccelarated flight)
Power_required=(CD*(w0/CL)*sqrt((2*w0)/(rho*CL*i)))/550; %Fundamentals of airship page 73
disp(Power_required)

%Thrust_required=CD*q*i;
Thrust_required=(Cadmin_total*q*i)+((K*(w0^2))/(q*i));
disp(Thrust_required)
%fprintf('Total CD is %f\n',CD)
Cl_needed=w0/(q*i);

%Take off Roll

T=7.46; %Dynamic thrust at 70.7 percent Vt0
prop_efficiency=0.6;
hp=1.006;

%T=(550*prop_efficiency*hp)/(2*(sqrt(w0/(i*rho*0.8*Cl_max))));
Fc=0.03; %Formula a=(g/W)[(T-D)-Fc(W-L)]; Sg=(Fv^2)/(2amean)
L=(0.5)*(rho)*((0.707*f_v)^2)*i*CLg;
area_drag=pi()*((d_fuse^2)/4);
%D=(0.5)*rho*((0.707*f_v)^2)*area_drag*(CD); %make change use frontal fuselage area
D=(0.5)*rho*((0.707*f_v)^2)*i*(CDg);

amean=(g/w0)*((T-D)-Fc*(w0-L));

Sg=(f_v^2)/(2*amean);

```

```

%fprintf('The take-off ground roll is %f ft\n',Sg)

%Rotation distance
Sr=0.5*fv;
%Transition distance, Str
R=(fv2)/((0.15)*g); %rotation distance
climb_rate=fv*((T-D)/w0); %Rate of climb
theta_cl=asin(((T-D)/w0));
%disp(theta_cl)
Str=R*sin(theta_cl); %transition distance
%fprintf('The transition distance is %f ft\n',Str)

%Climb distance
Htr=10;
Scl=(35-Htr)/tan(theta_cl);
climb_angle=theta_cl*180/pi;
%fprintf('Climb distance is %f ft\n',Scl)

%Total take off distance
takeoffdist_total=Sg+Sr;
%fprintf('Total takeoff distance is %f ft\n',takeoffdist_total)

%Time during take off
g_time=fv/amean; %Ground roll time
tr_time=(Str+(Scl/cos(theta_cl)))/(fv); %Transition distance time
total_time=g_time+tr_time;
%fprintf('Total time required for take-off is %f seconds\n',total_time)

%Landing Analysis (time req clear 50ft, free roll then brake to stop)
%NOTE Vs equal fv as w0 does not change and no flaps are used
Vs=fv/1.2; %Stall speed
V50=1.3*Vs;
Vtd=1.15*Vs;

%Air distance, Sa
Sa=(L/D)*(((V502)-(Vtd2))/(2*g))+50;
%fprintf('Air distance is %f ft\n',Sa)

%Free roll distance, Sfr
L_over_d=L/D;
%Braking distance, Sb
CLG=CLg; %airfoil dependent and landing config dependent
Sb=(w0/(g*Fc*rho*i*((CD/Fc)-CLG)))*log(1+(rho/2)*(i/w0)*((CD/Fc)-CLG)*(Vtd2));
%fprintf('Braking distance is %f ft\n',Sb)

%empty weight calculation
ref_density = 1.967;
aa_w = 0.2207; %airfoil dependent
aa_hw = 0.035019; %airfoil dependent
aa_vw = 0.094546; %airfoil dependent
wvol = aa_w*bw_w;
hwvol = aa_hw*bw_h;
vwvol = aa_vw*bw_v;
m_w = ref_density*wvol;
m_hw = ref_density*hwvol;
m_vw = ref_density*vwvol;
wm_total = (m_vw + m_w + m_hw)*1.2;
payload = w0 - 12 - wm_total;

```

```

if (wingsp <= 18) && (takeoffdist_total <= 100) && (Sb <= 400)
    flightscore(i)= 2^(1+(wingsp/5)) + payload/2;
    wings(i) = wingsp;
    emptyw(i) = wm_total;
    emptyw = wm_total;
    disp("Constraint was met")
    disp(T)
    fprintf("Wing area is %.2f ft^2\n", i)
    fprintf("Take-off roll distance is %.2f ft\n", Sg)
    fprintf("Total takeoff distance is %.2f ft\n", takeoffdist_total)
    fprintf("Breaking distance %.2f ft\n ", Sb)
    fprintf("Empty weight is %.2f lb\n ",emptyw)
else
    disp("Constraint was not met")
    disp(T)
    fprintf("Wing area is %.2f ft^2\n", i)
    fprintf("Take-off roll distance is %.2f ft\n", Sg)
    fprintf("Total takeoff distance is %.2f ft\n", takeoffdist_total)
    fprintf("Breaking distance %.2f ft\n ", Sb)
    fprintf("Empty weight is %.2f lb\n ",emptyw)
end
end
for j = 1:length(emptyw)
    if emptyw(j) ~= 0 %emptyw ~= 0
        fprintf("Empty weight is %.2f lb\n Wing Span %.2f ft\n Flightscore is %.2f", emptyw(j),wingsp(j),flightscore(i));
        %fprintf("Empty weight is %.2f lb\n Wing Span %.2f ft\n Flightscore is %.2f", emptyw,wingsp,flightscore);
    end
end
end

```

APPENDIX B: C_l vs α for S123 Airfoil

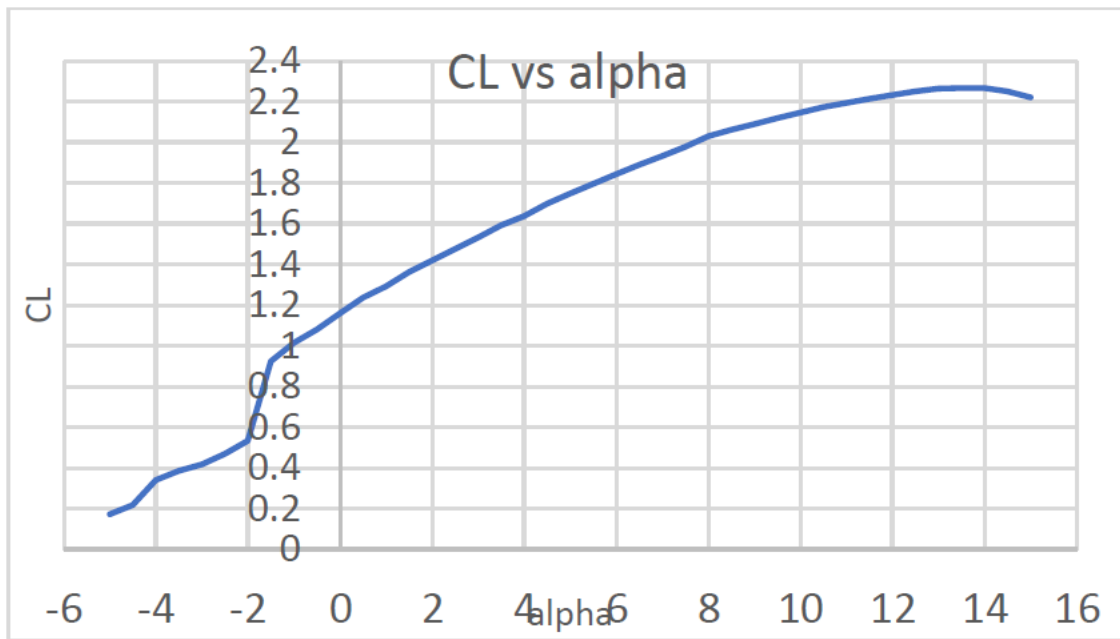


Figure 20: C_l vs α data for s1223 from XFLR5

APPENDIX C: Geometry File AVL

[Lancer1]

#Mach

0.0

#IYsym IZsym Zsym

0 0 0.0

#Sref Cref Bref

32 1.8551 17.8885

#Xref Yref Zref

0.0 0.0 0.0

!begingeometry

#=====

SURFACE

[Main wing]

!beginsurface

#Nchordwise Cspace Nspanwise Sspace

8 1.0 12 1.0

#

YDUPLICATE

0.0

#

ANGLE

-3.50

TRANSLATE

2.429 0.00000 0.00000

#-----

SECTION

!beginsection

#Xle Yle Zle Chord Ainc Nspanwise Sspace

0.0 0.0 0.0 2.3851 0.0 0.0 0.0

AFIL

s1223.dat.txt

!endsection

#-----

SECTION

!beginsection

#Xle Yle Zle Chord Ainc Nspanwise Sspace

0.35750 5.81376 0.0 1.67 0.0 0.0 0.0

AFIL

s1223.dat.txt

!endsection

#+++++

CONTROL

!begincontrol

```

#Cname Cgain Xhinge HingeVec SgnDup
Aileron 1.0 0.75 0.0 1.0 0.0 -1.0
!endcontrol
#-----
SECTION
!beginsection
#Xle Yle Zle Chord Ainc Nspanwise Sspace
0.596 8.945 0.0 1.1925 0.0 0.0 0.0
AFIL
s1223.dat.txt
!endsection
#+++++
CONTROL
!begincontrol
#Cname Cgain Xhinge HingeVec SgnDup
Aileron 1.0 0.75 0.0 1.0 0.0 -1.0
!endcontrol
!endsurface
#=====
SURFACE
[Horizontal Tail]
!beginsurface
#Nchordwise Cspace Nspanwise Sspace
8 1.0 12 1.0
#
YDUPLICATE
0.0
#
ANGLE
0.0
TRANSLATE
8.31 0.00000 0.00000
#-----
SECTION
!beginsection
#Xle Yle Zle Chord Ainc Nspanwise Sspace
0.0 0.0 0.0 1.0728 0.0 0.0 0.0
NACA
0009
!endsection
#+++++
CONTROL
!begincontrol
#Cname Cgain Xhinge HingeVec SgnDup
Elevator 1.0 0.65 0.0 1.0 0.0 1.0
!endcontrol
#-----
SECTION

```



```

!beginsection
#Xle Yle Zle Chord Ainc Nspanwise Sspace
0.0 3.75485 0.0 1.0728 0.0 0.0 0.0
NACA
0009
!endsection
#++++++
CONTROL
!begincontrol
#Cname Cgain Xhinge HingeVec SgnDup
Elevator 1.0 0.65 0.0 1.0 0.0 1.0
!endcontrol
!endsurface
SURFACE
[Vertical Tail]
!beginsurface
#Nchordwise Cspace Nspanwise Sspace
8 1.0 12 1.0
#
ANGLE
0.0
TRANSLATE
8.206 0.00000 0.00000
#-----
SECTION
!beginsection
#Xle Yle Zle Chord Ainc Nspanwise Sspace
0.0 0.0 0.0 1.3326 0.0 0.0 0.0
NACA
0009
!endsection
#++++++
CONTROL
!begincontrol
#Cname Cgain Xhinge HingeVec SgnDup
Rudder 1.0 0.65 0.0 0.0 1.0 1.0
!endcontrol
#-----
SECTION
!beginsection
#Xle Yle Zle Chord Ainc Nspanwise Sspace
0.0 0.0 2.6651 1.3326 0.0 0.0 0.0
NACA
0009
!endsection
#++++++
CONTROL
!begincontrol

```

```

#Cname Cgain Xhinge HingeVec SgnDup
Rudder 1.0 0.65 0.0 0.0 1.0 1.0
!endcontrol
!endsurface
!endgeometry

```

Appendix D: Mass File AVL

```

#[Lancer 1]
#Victor Ukiri, Date:2022/12/28
#x,y,z coordinate system matches AVL default
Lunit = 0.3048 m
Munit = 0.4535 kg
Tunit = 1.0 s
g = 9.81
rho = 1.1206 #at xkm above sea level, value matches value from density calc.
#fuselage length = 1 m
#mass x y z Ixx Iyy Izz
35 3.50 0 0 0 0 0 !Aircraftstructure
#El

```

Appendix E: Thrust Vs Velocity Graph

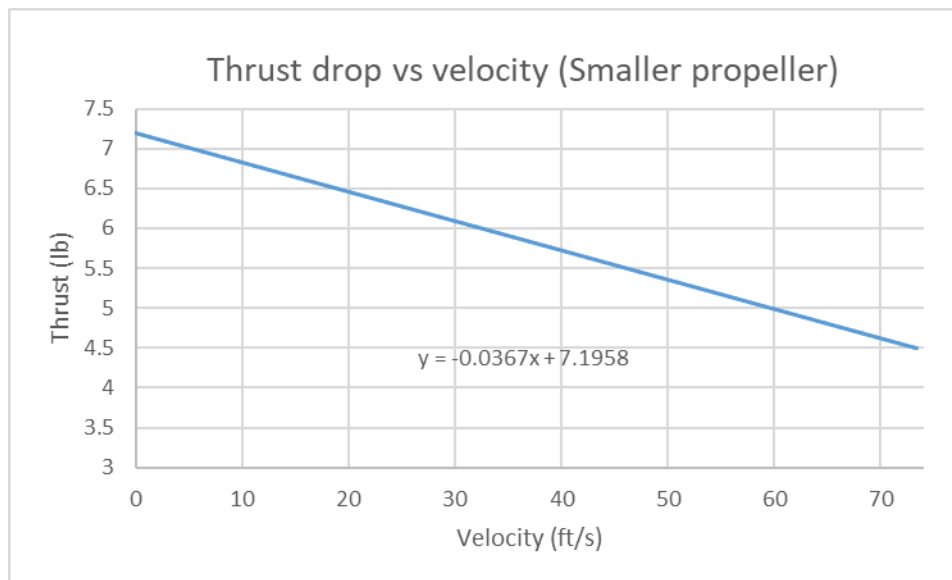


Figure 21: Thrust drop vs Velocity for Small Prop

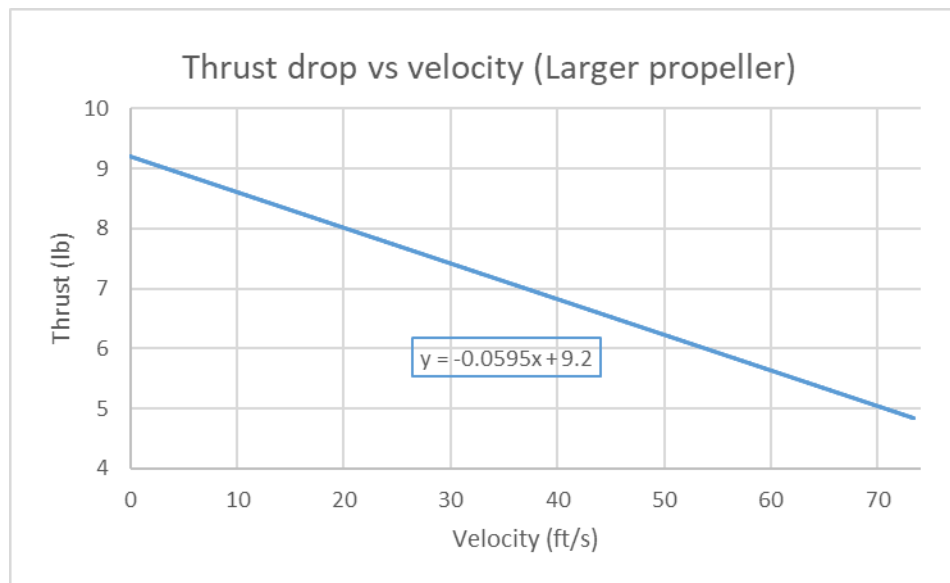


Figure 22: Thrust Drop vs Velocity for Large Prop

NOTE: Changing the propeller alone leads to an increase of 36 percent in payload capacity